



Since January 2020 Elsevier has created a COVID-19 resource centre with free information in English and Mandarin on the novel coronavirus COVID-19. The COVID-19 resource centre is hosted on Elsevier Connect, the company's public news and information website.

Elsevier hereby grants permission to make all its COVID-19-related research that is available on the COVID-19 resource centre - including this research content - immediately available in PubMed Central and other publicly funded repositories, such as the WHO COVID database with rights for unrestricted research re-use and analyses in any form or by any means with acknowledgement of the original source. These permissions are granted for free by Elsevier for as long as the COVID-19 resource centre remains active.



Disaster relief supply chain design for personal protection equipment during the COVID-19 pandemic

Behzad Mosallanezhad ^a, Vivek Kumar Chouhan ^b, Mohammad Mahdi Paydar ^{c,*},
Mostafa Hajiaghaei-Keshteli ^a

^a Tecnológico de Monterrey, Escuela de Ingeniería y Ciencias, Puebla, Mexico

^b Department of Mechanical Engineering, Indian Institute of Information Technology, Design and Manufacturing, Kanchepuram, Chennai, India

^c Department of Industrial Engineering, Babol Noshirvani University of Technology, Babol, Iran

ARTICLE INFO

Article history:

Received 23 January 2021
Received in revised form 7 August 2021
Accepted 10 August 2021
Available online 18 August 2021

Keywords:

Supply chain design
Personal protection equipment
COVID-19
Pandemic
Disaster relief supply chain

ABSTRACT

The global epidemic caused by novel coronavirus continues to be a crisis in the world and a matter of concern. The way the epidemic has wreaked havoc on the international level has become difficult for the healthcare systems to supply adequately personal protection equipment for medical personnel all over the globe. In this paper, considering the COVID-19 outbreak, a multi-objective, multi-product, and multi-period model for the personal protection equipment demands satisfaction aiming to optimize total cost and shortage, simultaneously, is developed. The model is embedded with instances and validated by both modern and classic multi-objective metaheuristic algorithms. Moreover, the Taguchi method is exploited to set the metaheuristic into their best performances by finding their parameters' optimum level. Furthermore, fifteen test examples are designed to prove the established PPE supply chain model and tuned algorithms' applicability. Among the test examples, one is related to a real case study in Iran. Finally, metaheuristics are evaluated by a series of related metrics through different statistical analyses. It can be concluded from the obtained results that solution methods are practical and valuable to achieve the efficient shortage level and cost.

© 2021 Elsevier B.V. All rights reserved.

1. Introduction

Reportedly, the COVID-19 pandemic became a severe infection with severe consequences, including detrimental respiratory system injuries and even death. Unfortunately, the number of infected cases worldwide is continuously increasing as of April 2021, according to the daily statistics about COVID-19 from World Health Organization (WHO). Evidence from different cases of the COVID-19 shows that it is spreading among people through close contact with an infected person and contaminated surfaces. Thus, societies experience a grave challenge in supplying medical necessities in a few days. Additionally, medical staff and healthcare personnel who have devoted their lives to serving the COVID-19 patients are at the highest risk of contamination [1]. A series of actions and measures have been taken and suggested by policymakers, governments, organizations, and healthcare systems against the COVID-19. These measures can be classified into different groupings, for instance, individuals, organizational, environmental, etc. [2].

One of the leading environmental measures is frequently cleaning and decontamination of surfaces with disinfectants like alcohol. Measuring body temperature, remote working, preventing

conferences and meetings, etc., are categorized as organizational measures [2]. Moreover, using Personal Protection Equipment (PPE) like face masks, social distancing, washing hands carefully and regularly, avoiding travel to busy high-risk areas, reduction of gathering like parties, and keeping away from hugging and kissing are some of the measures at individual levels [3,4].

Among mentioned measures, PPE meets the standard requirements to reduce the infection inhibition and losses caused by contagious viral diseases such as the COVID-19 and helps healthcare systems control the growth of the COVID-19 among their personnel. A group of PPEs is made to control personnel healthcare. The PPEs are gloves, gowns, respiratory protection, eye protection, and testing kits [5].

On the other side, the current stock of PPE might be quickly in shortage for many items like a medical mask or respiratory protection. This crisis is begun by the growing number of COVID-19 cases globally, alongside bulk buying of PPE due to misinformation and fear [1]. Moreover, PPE production has encountered diminished capacity, and increasing daily demand in the hospital must be met to care for contaminated patients [6]. Although it could be recommended numerous avenues to handle PPE demand befittingly, this study aims to propose a mathematical supply chain model in which optimal PPE flow in the network during the COVID-19 pandemic is critical.

* Corresponding author.

E-mail address: paydar@nit.ac.ir (M.M. Paydar).

Generally, emergency management has been defined in many ways. However, it can be summarized in three main aspects: being prepared before a disaster happens, immediate response to disasters, and reestablishing detrimental damages caused by natural or human-origin disasters [7]. Improper and meager care to injured people by disaster could bring about longstanding health impacts and fatality growth, specifically COVID-19. During a health disaster, adequate and timely supply of necessary commodities such as food, medicine, medical equipment has a tremendous impact on the hectic situation of the public health emergency [8].

In supply chain (SC) theories, the situation mentioned above is called supply chain disruption. Supply chain disruption is an unexpected occasion that disables one or more components in the supply chain and disrupts common goods and commodities distribution within the network [9,10]. Epidemic outbreaks are named as one of the particular cases of supply chain disruption that is consist of three features as follows: permanent presence and vague disruption level; concurrent disruption significantly spreads in supply chain and occurs over a broad population; it begins on a small scale and immediately dominates numerous geographic areas [11]. Emergency management practices' performance is intensively associated with relief supply chain design [12].

A set of consecutive activities which help to afford the material, produce goods, move production among the chain, and distribute the final products to their destination is defined as an SC [13]. Correspondingly, managing an SC is a set of applicable plans to handle the production cycle through numerous practices and integrate suppliers, producers, warehouses, and stores to produce and dispense the proper goods. At the same time, it optimizes costs and makes a competitive advantage available for all cooperated partners over the supply chain [14,15]. So, designing a relief SC is the center of focus, especially during a natural disaster or any uncertain medical emergency like COVID-19. The right step not taken on time becomes the reason for a large number of losses of lives.

Obviously, designing such relief SC networks under particular conditions like pandemic is inevitable to better response time and reliability. Safaei et al. [16] developed an efficient and cost-effective optimization framework to distribute relief items considering dynamic conditions adequately. Reportedly, the Chinese government built new medical facilities less than two weeks after understanding the COVID-19 outbreak in this country [17]. Similarly, the same approach has been implemented in several countries, like Iran, using churches, mosques, stadiums, etc., to be proactive to reach the following advantages:

- Supplying and delivering materials and drugs in the right quantity.
- Providing and planning the right number of nurses and doctors.
- Optimal transportation planning.
- Timely and well-organized responding to the patients.
- Proactive to possible future cases.
- Minimizing the total costs while servicing and covering all potential cases.
- Centralized decision-making.

Hence, this paper develops a multi-objective model including medical supply manufacturers, distributors, medical centers, and world donors to minimize both total costs and unsatisfied demand to provide better distribution of PPEs.

A detailed review of previous related works is conducted and reported in Section 2. The proposed model is formulated in Section 3. Section 4 provides the proposed solution approaches

and encoding scheme. We develop applied examples and computational results and also investigate a real case in Section 5. In Section 6, computational outputs are elaborated. Lastly, Section 7 embodies the conclusion is presented, and future directions are proposed.

2. Literature review

Recently, COVID-19 caused millions of death, and also this crisis has influenced global activities. Besides, economic troubles and malfunctions appeared in many sectors, including production, supply chain, logistics [32]. Since the universal supply chain has been dependent on China over the past decades, many large supply chain sectors, including those related to electronics and automotive industries, pharmaceutical manufacturers, airlines, transportation, etc., have been incredibly damaged by the COVID-19 outbreak [33].

As an authentic experience, before WHO's declaration about COVID-19 widespread presence, a global shortage in supplying PPE was abundantly noticeable. For instance, the storage of N95 masks in the United States reported by Health and Human Services (HHS) was only 12 million, considerably lower than what is expected to be the US needs. Moreover, the US government could not properly use domestic manufacturers to handle the PPE shortage of N95 masks. On the other hand, countries like South Korea made their domestic manufacturers allied to satisfy healthcare PPE demands [34].

Regarding the pandemic disruptions in the SC sector and mitigating severe and harmful impacts on different supply chains, researchers and scholars sought the presence of supply chains that can cope with the unpleasant troubles and problems in this field. As we elaborately discuss recent studies in the supply chain in following, they encompass a variety of subjects such as supply chain design [35,36], forecasting and planning [37], supply management [38,39], transportation and logistics management [40,41].

Nagurny [42] developed a supply chain network using mathematical modeling concentrated on labor availability during the COVID-19 pandemic for industries and businesses. In other researches considering COVID-19 circumstances, she and her collaborators also carried out studies on a variety of subjects, including presenting a model for demand competition on medical supplies and designing supply chain networks for perishable food [42–45].

Nandi et al. [46] suggested a resilient SC for COVID-19, which is subjected to transparency and sustainability. In this study, localization, agility, and digitization features have been considered in terms of SC. Ivanov [47] utilized simulation research toolkits to study the impacts of the virus on the chain worldwide. This research is divided into two parts. First, they clearly expressed why the epidemic led to a supply chain disruption then provided evidence supporting the practicability of simulation-based studies for predicting epidemic effects.

Goodarzi et al. [48] considered a sustainable chain related to COVID-19 conditions. They suggested a model facilitating medicine distribution to patients while finding the best way to produce and store medicine under perishability constraints. Since the proposed model is NP-hardness for large-size models, the authors decided to solve with hybrid meta-heuristics. In one of the devoting studies for the COVID-19, Abbasi et al. [49] designed an allocation model for a vaccination with both operational constraints (capacity of hospitals, transportation, and storage) and non-operational constraints (exposure risks).

In this work, we formulate an optimization problem for personal protection equipment during the pandemic. Hence, a brief survey on the relief supply chain design is presented, and the

Table 1
 Overview of relief supply chain literature.
 RSCN: Relief supply chain network
 PPD: Pre- and post-disaster.

Author(s)	Description	Period		Formulation			Applying Heuristics (Y/N)
		Single	Multi	Deterministic	Stochastic	Fuzzy	
Wang et al. [18]	They considered responses for a disaster in an RSCN (Walmart).	✓		✓			N
Nagurney and Nagurney [19]	They considered PPD relief products delivery.		✓		✓		N
Mohammadi et al. [20]	They developed a model to design an RSCN considering re-response emergency (The United States).		✓		✓		Y
Sung & Lee (2016)	They designed an RSCN to meet patients' demands	✓		✓			N
Zhou et al. [21]	They considered resources distribution in post-disaster by optimizing emergency resource allocation and scheduling.		✓	✓			Y
Jha et al. [22]	They designed an RSCN to distribute goods.	✓		✓			Y
Al Theeb and Murray [23]	They designed an RSCN considering VRP.		✓	✓			Y
Manopiniwes & Irohara (2017)	They considered PPD response in an RSCN.	✓			✓		N
Li et al. [24]	They considered supplies distribution in natural disasters (The United States)		✓	✓			N
Samani et al. (2018)	They considered blood distribution in RSCNs (Iran).		✓		✓	✓	N
Cao et al. [25]	They considered RSCN in natural disasters (China).		✓	✓			Y
Safaei et al. [16]	They considered logistics operations in RSCN (Iran).		✓		✓		N
Moreno et al. [26]	They designed a location-transportation model to make available relief aids to needy people. (A case study of 2011 based mega-disaster in Brazil).		✓	✓	✓		Y
Torabi et al. [27]	They presented an integrated relief model for the pre-position of the relief item to the planned location for pre-disaster agreements and post-procurement-related decision-making. (Iran).	✓			✓	✓	Y
Hong and Jeong [28]	They proposed a method for disaster planning.	✓		✓			N
John et al. (2019)	They modeled a humanitarian network in a food RSCN.	✓				✓	N
Sarma et al. [29]	The proposed model was a Facebook disaster map in emergency relief to identify the location of the victims; accordingly, the transportation plan, demand for the relief products are managed (India).	✓		✓			Y
Ghaffari et al. [7]	They considered an emergency-scheduling problem (India).	✓		✓			Y
Aghajani et al. [30]	They proposed a method to select the suppliers for a humanitarian RSCN (Iran).		✓		✓		N
Yenice and Samanlioglu [31]	Earthquake relief network presented to store and distribute relief aid to the people (Turkey)		✓		✓		N
This Study (2021)	Disaster RSCN for PPEs (Iran)		✓	✓			Y

more relevant literature on relief supply chain design is accessible in Table 1.

Habibi-Kouchaksaraei et al. [50] implemented a mathematical model for blood donation during disasters like earthquakes, floods. They utilized the goal programming technique to address their model. In some relief supply chain networks, finding the best location for distributing relief goods and telecommunication facilities is indispensable. Mohamadi et al. [51] figured this problem out as an optimization model based on multiple cases in a fuzzy environment. Their proposed model identifies the relevant places for telecommunication towers and shelters and assists decision-makers in amplifying the emergency services.

Shavarani [52] addressed one of the critical issues in disaster settings. When disaster happens, relief centers and gas stations are highly required not only for emergency services by organizations but also for the daily activities of individuals. He suggested mathematical modeling for a multi-level network. Akbarpour et al. [53] considered the same chain for pharmaceutical commodities. The robust optimization model has two objectives: one minimizes the cost of the relief network, and the other maximizes the demand coverage. The formulation also has considered

the uncertainty of demand, perishability of commodities, and mobility of facilities.

In one of the recent works of relief SC networks, Li et al. [54] tackled mathematical modeling to distribute injured parties and develop response networks. Ghasemi and Khalili-Damghani [55] presented a hybrid technique including simulation and mathematical modeling in uncertainty conditions for preparedness goals in the relief supply chain. This model cop with decisions regarding the setting up and allocation of distribution centers.

2.1. Research gap

Global COVID-19 outbreaks proved that a well-founded network must overcome unforeseen incidents and handle consequent events associated with the epidemic. One of the most reliable methods and the perfect way by which we can achieve the closest outputs to reality is mathematical modeling. In addition to its superiority in results, it can display a better tool for future prediction.

Literature reviews on COVID-19 supply chain studies and relief SC are presented in the previous section and Table 1 to ensure the

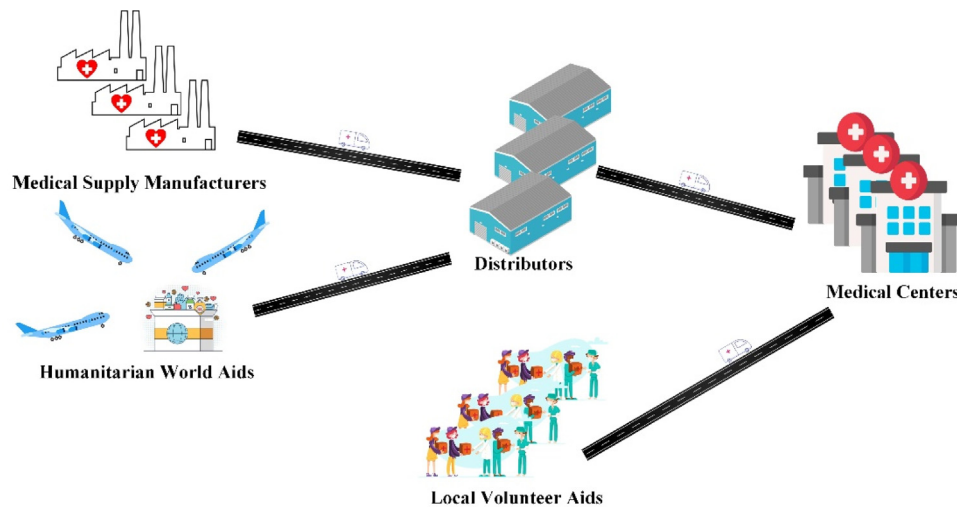


Fig. 1. COVID-19 PPE supply chain network.

developed model is unique in terms of novelty and application. Most of the previous works in the COVID-19 supply chain are focus on subjects comprising labor availability of supply chain, medical supply chain, and allocation model for vaccination. On the other hand, designed relief supply chain literature has paid attention to problems such as blood donation, emergency services, and pharmaceutical distributions.

The proposed bi-objective, multi-period, and multi-product deals with the total cost and unsatisfied demands minimization. No study reported the fair distribution of PPEs among medical centers of a region, considering medical supply manufacturer, distributor, medical center, and world donator. Therefore, there is no similar model for PPE distribution in this context; this model can help prominent associations and organizations to control the COVID-19 pandemic situation.

3. Problem definition and formulation

Generally, there are three primary sources, medical supply manufacturers, humanitarian world aids, and local volunteer aids, to supply and satisfy the PPE demand of the healthcare system, as shown in Fig. 1. These purchased commodities from medical supply manufacturers (MSMs) or globally dispatched medical aids are directly moved to the distributors. Generally, the distributors are authorized institutes or organizations by governments or the ministry of health and medical education. However, local aids are straightly donated to outpatient clinics or hospitals. They are responsible for allocating needed PPE to be occupied and selected hospitals for COVID-19 patients.

One of the pillars of any SC network, especially a relief SC network, is controlling costs or making more profit. According to the literature review, cost minimization is one of the organizations' essential goals, so most studies in this context have employed a cost minimization objective [56,57]. Moreover, a relief chain may confront unsatisfied demands, known as a shortage of demands. With this in mind, to model the relief supply chain existence of fairness for demand shortage is essential [58,59]. Consequently, for the second objective function of this study, we aim to minimize unsatisfied demands.

3.1. Mathematical modeling

In this section, the proposed network is formulated by a mathematical modeling approach.

Indices

i	MSM center ($i = 1, \dots, I$)
j	Distributor ($j = 1, 2, \dots, J$)
c	COVID-19 PPE ($c = 1, 2, \dots, C$)
h	Medical center ($h = 1, 2, \dots, H$)
w	World donator ($w = 1, \dots, W$)
t	Time periods ($t = 1, \dots, T$)

Deterministic parameters

S_c	Occupied space by storing per PPE c (m^3)
$Caps_{ict}$	The maximum amount produced PPE c by MSM i in period t
$Capd_j$	The capacity of distributors j (m^3)
WD_{wct}	The maximum donation of PPE c by world donator w in period t
VA_{hct}	The number of donated PPE c by voluntary in period t to medical center h
CDH_{jhc}	Transportation cost of PPE c from distributors j to medical center h
CMD_{ijc}	Transportation cost of PPE c from MSM i to distributors j
CMD_{wjc}	Transportation cost of PPE c from world donator w to distributors j
hd_{jc}	Inventory holding cost for PPE c charged by distributor j
PC_{cit}	The procurement cost for PPE c charged by supplier i in period t

Demand parameters

F_h	The treatment capacity of medical center h
IR_t	COVID-19 Infection percentage during period t
Pop	Population of region
MP	Percentage of needed medical center personnel per COVID-19 patients
TP_{ht}	Number of COVID-19 patients in treatment in medical center h during period t
RP_{ht}	The recovery rate of COVID-19 patients in medical center h during period t
DP_{ht}	Death rate COVID-19 patients in medical center h during period t
SH_{ht}	Number of working shifts in medical center h in period t
RU_c	Number of times that PPE c can be reused
D_{hct}	Demand for PPE c in medical center h during period t

$$D_{hct} = \left(\left[\frac{(Pop \times IR_t \times F_h)}{\sum F_h} + TP_{ht}(1 - RP_{ht} - DP_{ht}) \right] \times MP \times SH_{ht} \right) \times \frac{T}{RU_c}$$

Flow Decision Variables

XMD_{ijct}	Number of PPE c shipped from MSM i to distributor j in period t
XWD_{wjct}	Number of PPE c shipped from world donator w to distributor j in period t
XDH_{jhct}	Number of PPE c shipped from distributor j to medical center h in period t

Inventory Decision Variables

IDW_{jct}	The number of PPE c in distributor j in period t
B_{hct}	Unsatisfied demand for PPE c in period t

Assignment Decision Variables

DW_{jh}	Is 1 if Distributor j is assigned to medical center h otherwise 0
-----------	---

Objective Functions

$$\begin{aligned} \text{Min } Z_1 = & \sum_i \sum_j \sum_c \sum_t CMD_{ijc} XMD_{ijct} \\ & + \sum_w \sum_j \sum_c \sum_t CMD_{wjc} XWD_{wjct} \\ & + \sum_j \sum_h \sum_c \sum_t CDH_{jhc} XDH_{jhct} \\ & + \sum_j \sum_c \sum_t hd_{jc} IDW_{jct} + \sum_i \sum_j \sum_c \sum_t PC_{cit} XMD_{ijct} \end{aligned} \tag{1}$$

$$\text{Min } Z_2 = \sum_c \sum_t \max_{h \in H} \{B_{hct}\} \tag{2}$$

Eq. (1), as the first objective function, is to minimize the cost of the PPE supply. It includes four parts: the first to third part concentrate on transportation costs between different network components, while the fourth calculates holding cost in distribution spots. The second objective function (Eq. (2)) makes the model distribute the PPE in the network equitably to optimize the maximum amount of unsatisfied demands. Interested readers might refer to the [Appendix](#) for linearizing the second objective function (Eqs. (A.1) and (A.2)).

Constraints

$$\sum_j XDH_{jhct} + VA_{hct} + B_{hct} = D_{hct} \quad \forall h, c, t \tag{3}$$

$$\sum_i XMD_{ijct} + \sum_w XWD_{wjct} = IDW_{jct} + \sum_h XDH_{jhct} \quad \forall j, c, t = \{1\} \tag{4}$$

$$\sum_i XMD_{ijct} + \sum_w XWD_{wjct} + IDW_{jct-1} = IDW_{jct} + \sum_h XDH_{jhct} \quad \forall j, c, t \tag{5}$$

$$\sum_j XWD_{wjct} \leq WD_{wct} \quad \forall w, c, t \tag{6}$$

$$\sum_j XMD_{ijct} \leq Caps_{ict} \quad \forall i, c, t \tag{7}$$

$$\sum_c IDW_{jct} \times S_c \leq Capd_j \quad \forall j, t \tag{8}$$

$$\sum_j DW_{jh} \geq 1 \quad \forall h \tag{9}$$

$$\sum_c XDH_{jhct} \leq M \times DW_{jh} \quad \forall j, c, t \tag{10}$$

$$DW_{jh} \leq \sum_c \sum_t XDH_{jhct} \quad \forall j, h \tag{11}$$

$$XMD_{ijct}, XWD_{wjct}, XDH_{jhct}, IDW_{jct}, B_{hct} \geq 0 \quad \forall i, j, w, h, c, t \tag{12}$$

$$DW_{jh} = \{0, 1\} \quad \forall j, h \tag{13}$$

Constraint (3) checks the demand flow between the distribution centers and medical centers. B_{hct} is a positive decision variable for the shortage of demand in this flow, provided the transported PPE to the medical center does not match the exact amount of demand. Constraints (4) and (5) control the distribution centers' inventory level and balance the PPE input and output. Constraints (6)–(8) are capacity constraints. Constraint (6) imposes that the total amount of PPE transported from world donators to distribution cannot be unlimited, and it must be less than or equal to the maximum donation by world donators. Constraint (7) denotes that the total amount of PPE moved between the medical manufacturer and distribution centers are limited to each manufacturer's highest production capacity. Constraint (8) is a space constraint that ensures that distribution centers have sufficient space to conserve PPE packages. Constraint (9) make at least one distribution center to be established. The products might be transported to medical centers from distribution spots only if they are opened, guaranteed by constraint (10). Correspondingly, constraint (11) ensures that there will be PPE transportation flow between distribution spots and medical centers if assigned to each other. Constraint (12) specifies PPE transportation between nodes, inventory variables for distribution centers, and demand shortage in medical centers. Also, constraint (13) ensures the assignment of binary variables.

4. Solution approach

The following section is divided into two subsections: encoding strategy and multi-objective algorithms. The first subsection deals with the utilized encoding scheme known as the random-key method [60,61]. In the second subsection, four metaheuristics are developed, including some famous and recent algorithms in addition to hybrid ones.

4.1. Encoding strategy

The random-key method is a popular technique to generate the chromosome size for any problem. The generated chromosome will be in the form of a matrix that represents the set of candidate solutions. These chromosomes are then sorted, and priorities are assigned. The matrix obtained after that is known as the priority-based matrix. Initially, the set of candidate solutions are generated in the interval (0, 1) based on the considered problem size. This proposed chromosome matrix, as shown in Fig. 2, is generated by assuming the following data: Medical supply manufacturers (i) = 2, Humanitarian world aids (w) = 3, Distributors (j) = 3, Medical centers (h) = 2, and, time period = 4.

The chromosome matrix designed has two components according to the designed chromosome structure $i + w + 2 \times j + h$. This chromosome matrix is then converted to the priority-based matrix by assigning the priorities to the random keys, as shown in Fig. 3. Based on these priorities, the flow decisions will be taken. From Fig. 3(a), component one depicts the flow of relief aids from second medical supply manufacturers and humanitarian world aids to the third distributors. This process goes on till one of the capacities is exhausted. When this happens, a second facility is selected, and the procedure is repeated for the other. Similarly, Fig. 3(b) illustrates the flow of received goods from the first medical centers' first distributors.

4.2. Multi-objective algorithms

Generally, these algorithms are to find an optimal solution between two or more conflicting objectives. The weighted sum approach is a famous solution approach in a multi-objective perspective [36,62–64]. Under this method, initially, all the objectives are converted to single-objective by assigning some weight, making it easier to apply traditional algorithms. The decision-makers choose the objective function and weight assignments according to the preference of the utility. In contrast, using the Pareto optimal concept achieves a non-dominance solution rather than converting the original problem to a single-objective one [48,65–67]. These non-dominance solutions can be determined through comparisons of solutions obtained from the Pareto Front.

The Pareto optimal solution shows good trade-offs between objectives, due to which it is seen as a preferred solution. Pareto fronts are particularly non-dominating solutions that are necessary for this trade-off. Like if we consider two solutions, X and Y. Furthermore, the crowding distance calculation is used to select a good solution from the obtained front.

4.2.1. Multi-Objective Keshtel Algorithm (MOKA)

The MOKA is a well-known metaheuristics algorithm. The algorithm was first introduced and developed by Hajiaghaei-Keshteli and Aminnayeri [68,69]. In the proposed algorithm, the merging of the population is done based on the sorting using the crowding distance. The procedure is shown in Fig. 4. In this algorithm, Keshtel is referred to as randomly generated solutions, the food source is the solution, and the lake is the feasible region.

The algorithm follows the six main steps:

1. *Landing of the Keshtels in the lake*: randomly generated solutions.
2. *Finding the lucky Keshtels*: finding better solutions in terms of solution quality.
3. *Attraction and swirling*: local search.
4. *Moving Keshtels*: to cover the unexplored regions.
5. *Startling the Keshtels*: replacing the worst solution with new randomly generated solutions.

More explanations can be found in Cheraghali-pour et al. [70], and the pseudo-code is presented in Fig. 5.

4.2.2. Multi-objective Simulating Annealing (MOSA)

The process of this algorithm, which its basic version is firstly proposed by Kirkpatrick et al. [71], can be defined as firstly keeping the maximum temperature for the heat bath at which the solid melts. At this temperature, the particles arrange them randomly, and later, the temperature is decreased slowly and carefully. At last, the solid structure is arranged in the optimal lattice structure with minimum energy. Here T is the maximum temperature of the heat bath, α is the Boltzmann constant, and the accepting rule is known as the Metropolis criteria. The interested readers may refer to Cheraghali-pour et al. [70]. The pseudo-code of the MOSA is illustrated in Fig. 6.

4.2.3. Non-dominated Sorting Genetic Algorithm II (NSGA-II)

Genetic Algorithm (GA) is known as one of the most efficient algorithms to solve a wide range of the problem developed by Holland (1975). The multiple objective genetic algorithms MOGA is a particular case when the problem has various objectives. The diversity in the algorithm is maintained using the crowding distance sorting to the set of made solutions [72]. Finally, it converges and returns the optimal Pareto front. To study more, see Deb et al. [73]. Fig. 7 illustrates the pseudo-code of this algorithm.

4.2.4. Hybrid Multi-objective Keshtel Algorithm and Simulating Annealing (MOKASA)

The proposed hybrid MOKASA is designed to enrich the search phase of the KA by hybridizing with the SA algorithm intelligently. The generated population in KA gets divided into three parts such as N_1, N_2 and, N_3 . The N_1 the population is known as the best solution and N_3 is known as the worst solution. The algorithm has an intense exploration phase and during the exploitation phase the N_3 the population is generated randomly using the SA. The better solution witnessed will be accepted or rejected based on the Metropolis criteria. The interested readers may also refer to Chouhan et al. [60]. Fig. 8 illustrates the pseudo-code of this algorithm.

5. Applied examples

Although the number of cases shockingly increases, according to official Iranian statistics provided by the Ministry of Health and Medical Education,¹ more than 2,006,964 COVID-19 cases are confirmed, in which 63,884 cases are dead, and 1,684,570 cases are recovered until 8th April 2021. Still, the country has an increasing number of total cases; but the right step was taken at the correct time to ensure the total cases are significantly less as compared to the other countries such as Italy, USA, France, Spain, Germany, UK, Russia, Turkey, etc.² Countries such as France and Italy, known for their world-class health care facilities, are also failed to do the needful for the country's people.³

¹ <https://behdasht.gov.ir/>.

² <https://www.worldometers.info/coronavirus/>.

³ <https://www.who.int/healthinfo/paper30.pdf>.

Period	Component 1						Component 2						
	<i>i+w</i>			<i>j</i>			<i>j</i>			<i>h</i>			
	1	2	1	2	3	1	2	3	1	2	3	1	2
1	0.8147	0.6323	0.9575	0.9271	0.4217	0.6557	0.4787	0.0534	0.2769	0.6948	0.4387	0.1868	0.7093
2	0.9057	0.0975	0.9648	0.4853	0.9157	0.0357	0.7577	0.1711	0.0461	0.3170	0.3815	0.4897	0.7546
3	0.1269	0.2784	0.1576	0.8002	0.7922	0.8491	0.7431	0.7060	0.0971	0.9502	0.7655	0.4455	0.2760
4	0.9133	0.5468	0.9705	0.1418	0.9594	0.9339	0.3922	0.0318	0.8234	0.0344	0.7952	0.6463	0.6797

Fig. 2. The proposed chromosome structure.

Period	Component 1						Component 2								
	<i>i+w</i>			→	<i>j</i>			→	<i>j</i>			<i>h</i>			
1	2	1	3		2	1	3		2	1	1	3	2	1	2
2	2	2	3		1	2	1		3	2	1	2	3	1	2
3	1	3	1		3	2	3		2	1	1	3	2	2	1
4	2	4	3		1	2	3		2	1	3	1	2	1	2

(a) (b)

Fig. 3. The assigned priorities for (a) component 1 and (b) component 2.

```

N = |F| //number of solutions in F
For i = 1, ... .. N
    F[i]distance = 0 //initialize distance
End for
For m = 1 ... .. M //number of objective functions
    Sort (F, m) //sort using each objective function
    F[1]distance = F[N]distance = ∞ // boundary solutions are always selected
    For i = 2 ... .. (N - 1) //For all other points
        
$$F[i]_{distance} = F[i]_{distance} + \left( \frac{F[i + 1].m - F[i - 1].m}{f_m^{max} - f_m^{min}} \right)$$

    End for
End for
    
```

Fig. 4. Crowding distance procedure.

The instances are probed and investigated to validate the model's pertinence and solution approach in this section. In this regard, we developed fifteen test problems in different sizes (Table 2). The third example is evolved from a real case. Khuzestan

province in southern Iran is marked as red zones in Iran with 16,632 Positive cases, 613 deaths, and 15,309 recovered cases until 3rd June 2020. In all examples, we assume that the network

MOKA pseudo-code	
1	Land N Keshtel and calculate fitness
2	Do non-dominate shorting and calculate crowding distance
3	Again, sort the non-dominated Keshtels based on crowding distance
4	Find lucky Keshtels
5	Find best Lucky Keshtel (<i>LK</i>)
6	For each lucky Keshtels (N_1)
6.1	Nearest Keshtel (<i>NK</i>) keep on Swirl around the <i>LK</i>
6.2	In case better food is obtained, <i>NK</i> replaces <i>LK</i> . For new <i>NK</i> go to step 6.1
6.3	Excess food available attracts <i>NK</i> do swirling else go to step 8
7	<i>LKs</i> explores the unexplored regions for the existence of food.
8	The Keshtels with the least food are replaced with new Keshtels (N_3)
9	Move the remaining Keshtels in the lake between the other Keshtels (N_2)
10	Merge the population [$N_1; N_2; N_3$]
11	Do non-dominate shorting and crowding distance
12	Again, sort the non-dominated Keshtels based on crowding distance
13	Select (<i>N</i>) better Keshtels from this merged population for the next generation
14	Do steps 11 and 12 for the new population
15	Stop if stopping criteria meet; otherwise, go to step 5

Fig. 5. The MOKA pseudo-code.

MOSA pseudo-code	
1	Initialize and evaluate the fitness value ($x, f_j(x)$) Where, $\Delta f_j = f_j(x') - f_j(x), j = 1, 2 \dots \dots J$
2	Best solution = ($x, f_j(x)$)
3	For $i = 1$ to <i>max iteration</i>
3.1	Do mutation operator x'
3.2	Calculate the fitness value and (Δf_j)
3.2.1	If $\Delta f_1 \leq 0 \ \&\& \ \Delta f_2 \geq 0$ Update the best solution = ($x', f_j(x')$) Update the solution $x = x'$
3.2.2	Else if $\Delta f_1 \geq 0 \ \&\& \ \Delta f_2 \geq 0 \ \parallel \ \Delta f_1 \leq 0 \ \&\& \ \Delta f_2 \leq 0$ Keep the solution Pareto set
3.3.3	Else $\Delta f_1 \leq 0 \ \&\& \ \Delta f_2 \leq 0$ $P_1 = \exp\left(\frac{-\Delta f_1}{T}\right), P_2 = \exp\left(\frac{-\Delta f_2}{T}\right), h = rand$ If $h < P_1 \ \&\& \ h < P_2$ Update the solution $x = x'$
4	Update temperature ($T = \alpha * T$)
5	Do non-dominated sorting of the Pareto set
6	Stop if stopping criteria meet otherwise, go to step 3.1

Fig. 6. The MOSA pseudo-code.

is designed to handle PPE demands for four time periods, each of which is seven days.

In the real-case example, two medical supply manufacturers qualified by the ministry of health and medical education are active in Khuzestan, one in Khorramshahr, and one in Ahvaz. In addition, two international channels, the international Ahvaz airport and Bandar-e-Emam international port exist in Khuzestan to receive international donations. During COVID-19

outbreaks, the government of Iran exclusively appointed medical sciences universities to store and distribute both purchased and global donated PPE. Therefore, in Khuzestan, five medical sciences universities are responsible for supplying necessary PPE for COVID-19 medical centers all over the province. In a similar situation, ten particular medical centers throughout the province are planned to serve the COVID-19 patients. Lastly, the medical centers require a wide range of different PPE; nevertheless, the

NSGA-II pseudo-code

```

1 Initialize the random population
2 Calculate the fitness value
3 Non-dominance ranking is assigned to the individuals
4 While  $It \leq MaxIt$ 
5   Reproduce the population of offspring
6   Do selection, crossover, and mutation
7   Fitness values are calculated
8   populations are merged
9   Non-dominance ranking is assigned to the individuals
10  Non-dominated Pareto fronts sets are created
11  Between the points on each front, crowding distances are calculated
12  Based on the ranks and crowding distance, new parents are selected
13  Pareto optimal solutions are stored
14   $It = It + 1$ 
15 End while

```

Fig. 7. The NSGA-II pseudo-code.

Algorithm 4

```

1 Land N Keshtel and calculate fitness
2 Do non-dominate shorting and calculate crowding distance
3 Again sort the non-dominated Keshtels based on crowding distance
4 Find lucky Keshtels
5 Find best Lucky Keshtel ( $LK$ )
6 For each lucky Keshtels ( $N_1$ )
6.1 Nearest Keshtel ( $NK$ ) keep on Swirl around the  $LK$ 
6.2 In case better food is obtained,  $NK$  replaces  $LK$ . For new  $NK$  go to step 6.1
6.3 Excess food available attracts  $NK$  do swirling else go to step 8
7  $LK$ s explores the unexplored regions for the existence of food.
8 The Keshtels with the least food are replaced with new Keshtels ( $N_3$ )
9 Accept ( $x'$ ) as a new solution if its objective is better than ( $x$ )
10 % SA Main loop
10.1 Else if  $\Delta f_1 \leq 0 \ \&\& \ \Delta f_2 \geq 0$ 
10.2 Update the best solution = ( $x', f_j(x')$ )
10.3 Update the solution  $x = x'$ 
10.4 Else if  $\Delta f_1 \geq 0 \ \&\& \ \Delta f_2 \geq 0 \ \parallel \ \Delta f_1 \leq 0 \ \&\& \ \Delta f_2 \leq 0$ 
10.5 Keep the solution Pareto set
10.6 Else  $\Delta f_1 \leq 0 \ \&\& \ \Delta f_2 \leq 0$ 
10.7  $P_1 = \exp\left(\frac{-\Delta f_1}{T}\right), P_2 = \exp\left(\frac{-\Delta f_2}{T}\right), h = rand$ 
10.8 If  $h < P_1 \ \&\& \ h < P_2$ 
10.9 Update the solution  $x = x'$ 
10.10 Update temperature ( $T = \alpha * T$ )
11 Merge the population [ $N_1; N_2; N_3$ ]
12 Do non-dominate shorting and crowding distance
13 Again, sort the non-dominated Keshtels based on crowding distance
14 Select ( $N$ ) better Keshtels from this merged population for the next generation
15 Do steps 12 and 13 for the new population
16 Stop if stopping criteria meet otherwise, go to step 5

```

Fig. 8. Pseudo-code of the MOKASA.

Table 2
Fifteen test problems with various ranges of dimensions.

Test #	Indices					
	<i>i</i>	<i>w</i>	<i>j</i>	<i>c</i>	<i>h</i>	
Small-Size	1	2	2	3	4	2
	2	3	3	4	5	7
	3	2	2	5	6	10
	4	8	9	7	6	10
	5	10	10	8	9	12
Medium-Size	6	14	13	12	10	14
	7	17	12	16	10	15
	8	20	14	18	12	20
	9	24	14	22	14	22
	10	27	20	30	14	25
Large-Size	11	36	20	48	16	40
	12	40	25	50	16	50
	13	60	25	52	18	63
	14	56	30	60	20	74
	15	70	30	64	20	80

shortage of apron protection, surgical gloves, face shields, respirator, surgical gowns, and masks are pretty tangible in Khuzestan. Because of the strange situation with which medical centers and related organizations are dealing, the needed data are not provided precisely. As a result, the data are presented in approximate form in Table 3, retrieved from the Statistical Center of Iran,⁴ and the Ministry of Health and Medical Education. Fig. 9 is a symbolic scheme for medical supply manufacturers, world donators, distributors, and medical centers in Khuzestan province.

6. Computational results

In the subsequent section, we explore parameter tuning and the behavior of the proposed multi-objective algorithm using the different assessment metrics. To verify the obtained results from the proposed algorithm, statistical techniques have been utilized.

⁴ <https://www.amar.org.ir/english>.

Table 3
Model parameters ranges.



Parameter	Values	Parameter	Values
S_c	Uniform ~ [1, 2]	PC_{cit}	Uniform ~ [200, 5000]
Cap_{sict}	Uniform ~ [20, 42]	F_h	Uniform ~ [100, 700]
Cap_d_j	Uniform ~ [300, 700]	IR_t	Uniform ~ [0.001, 0.01]
WD_{wct}	Uniform ~ [15, 50]	Pop	Uniform ~ [1000, 30000]
VA_{hct}	Uniform ~ [0, 10]	MP	Uniform ~ [0.025, 0.05]
CDH_{jhc}	Uniform ~ [2, 20]	TP_{ht}	Uniform ~ [0.7, 0.95] × F_h
CMD_{ijc}	Uniform ~ [40, 1000]	RP_{ht}	Uniform ~ [0.1, 0.5]
CWD_{wjc}	Uniform ~ [20, 60]	DP_{ht}	Uniform ~ [0.1, 0.3]
hd_{jc}	Uniform ~ [2, 5]	SH_{ht}	2,3
RU_c	Uniform ~ [1, 10]		

6.1. Performance metrics

After reaching tuned levels for each algorithm, the proposed algorithms are set with these tuned control parameters to find the optimal results. The performance measures for multi-objective problems are somewhat different from single-objective problems. Multiple studies proposed numerous measures to appraise the multi-objective metaheuristics' performance and help scholars identify intelligent algorithms rather than others. Typically, performance matrices are used to analyze Pareto fronts. Thus, this study utilizes specific metrics to appraise multi-objective metaheuristics added to the next section. The interested reader may also refer to Behnamian and Ghomi [74], Fard et al. [75], and Roghanian and Cheraghalipour [76].

6.1.1. Spread of non-dominated solution (SNS)

SNS calculates the spread of ideal and non-dominance solutions by the following formula:

$$SNS = \sqrt{\frac{\sum_{i=1}^n (\bar{c} - c_i)^2}{n - 1}} \tag{14}$$

Here, $c_i = \left\| \vec{f}_i - \vec{f}_{Ideal} \right\|$, $\bar{c} = \frac{c_i}{n}$, $\vec{f}_{Ideal} = \{ \min(f_1), \min(f_2), \dots, \min(f_k) \}$

6.1.2. Mean ideal distance (MID)

In order to find the gap between Pareto and the ideal solution, we utilize this index, and obviously, the lesser MID is always preferred to achieve better performance.

$$MID = \frac{\sum_{i=1}^n \sqrt{\left(\frac{f_{1i} - f_{1}^{best}}{f_{1,max} - f_{1,min}} \right)^2 + \left(\frac{f_{2i} - f_{2}^{best}}{f_{2,max} - f_{2,min}} \right)^2}}{n} \tag{15}$$

where n represents the entire non-dominated set.

6.1.3. Maximum Spread (MS)

The distance between solutions is calculated by this index concerning the best Pareto front and is given as:

$$MS = \frac{1}{M} \sum_{m=1}^M \left(\frac{\min(F_{i,known}^{max}, F_{i,true}^{max}) - \max(F_{i,known}^{min}, F_{i,true}^{min})}{F_{i,true}^{max} - F_{i,true}^{min}} \right)^2 \tag{16}$$

M represents the total objective considered, $F_{i,known}^{max}$ and $F_{i,known}^{min}$ represent the maximum and minimum of i th function value in F_{known} respectively, $F_{i,true}^{max}$ and $F_{i,true}^{min}$ represents the maximum and minimum of i th function value in F_{true} , respectively.

6.1.4. Hypervolume (HV)

If the points are represented as a solution in the objective space, the solution set's n -dimensional space (or volume) is referred to as hypervolume. In other words, hypervolume is a metric that measures the volume covered by Pareto set in the feasible space for the objective function. Hypervolume is calculated according to Eq. (17),

$$HV = volume \left(\bigcup_{i=1}^{|R|} b_i \right) \tag{17}$$

where R is the set of Pareto solutions, b_i is volume regarding a reference point T .

6.1.5. CPU time

An important factor for evaluating an algorithm's performance is the speed of running the algorithm that achieves optimal solutions. The CPU time for any algorithm is the total computational time for that algorithm. According to this metric, always lesser CPU time is preferred.

Table 4

The algorithms' parameters and their levels.

Metaheuristics	Parameter	Parameter Level			Optimum Level
		L1	L2	L3	
NSGA-II	Max_{it}	100	200	300	100
	N_{pop}	100	150	200	150
	P_c	0.7	0.75	0.8	0.8
	P_m	0.05	0.10	0.15	0.05
MOSA	Max_{it}	100	200	300	200
	T_0	1000	1500	2000	1000
	T_{damp}	0.88	0.90	0.99	0.90
MOKA	Max_{it}	100	200	300	100
	N -Keshstel	100	150	200	100
	S_{max}	10	15	20	15
	$M1$	0.05	0.1	0.15	0.05
MOKASA	$M2$	0.2	0.25	0.30	0.30
	Max_{it}	100	200	300	200
	N -Keshstel	100	150	200	100
	S_{max}	10	15	20	15
	$M1$	0.05	0.1	0.15	0.15
	$M2$	0.2	0.25	0.30	0.25
	T_0	1000	1500	2000	1500
T_{damp}	0.88	0.90	0.99	0.90	

6.2. Parameters tuning

Before further proceeding, to avoid useless and time-consuming runs of metaheuristics, parameters are carefully tuned using a popular design of experiment (DOE) method. Among various DOE techniques, Taguchi experimental design method is selected. This method was developed by Taguchi [77]. Taguchi method seeks for maximization of controllable factors as well as minimization of noise effect. In various circumstances, this ratio is considered better in one of these three cases: smaller, nominal, and larger. Since our model is a minimization problem, tuning of parameters is attained by "the smaller is better" for each algorithm (see Eq. (18)).

$$S/N = -10 \times \log \left(\sum (Y^2)/n \right) \tag{18}$$

In this study, the response value is computed based on the division of two separated metrics, namely MID and MS (Eq. (19)).

$$MCOV = MID/MS \tag{19}$$

This response value considers both the convergence rate of solution (MID) and verity of solution (MS) [70]. For a start, the level of each factor for different algorithms should be identified. MOSA has three parameters with three levels. NSGA-II and MOKA have four and five parameters with three levels, respectively. Finally, MOKASA contains seven parameters with three levels. Thus, L_{27} is recommended as a proper array for NSGA-II, MOKA, and MOKASA in addition to L_9 for MOSA. For tuning purposes, test number 10 in Table 2 is applied. Then, the orthogonal arrays are implemented in Minitab software. The obtained plot of S/N is shown in Figs. 9–12. According to this S/N ratio plot, the level of parameters with the lowest value is preferable. Additionally, tuned values for the tenth test reported in Table 4 are considered for all test problems.

6.3. Comparison among algorithm

In this section, a comprehensive comparison is presented to check the quality of performance for each algorithm. To this end, we use five performance metrics. In the beginning, we set the parameters with the tuned values obtained in the previous section, then run each test problem 30 times and reported the

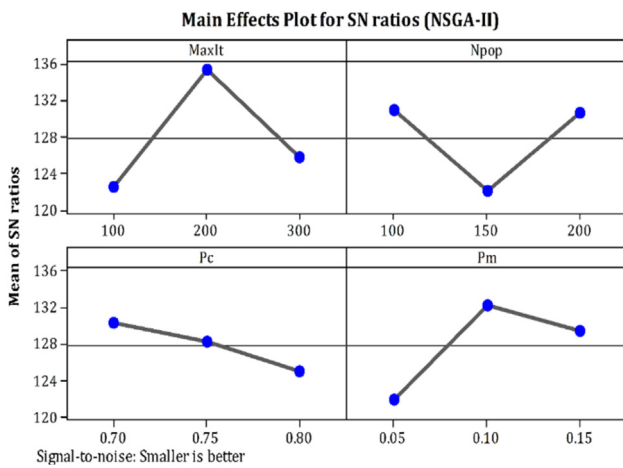


Fig. 9. Signal to Noise ratio plot for NSGA-II.

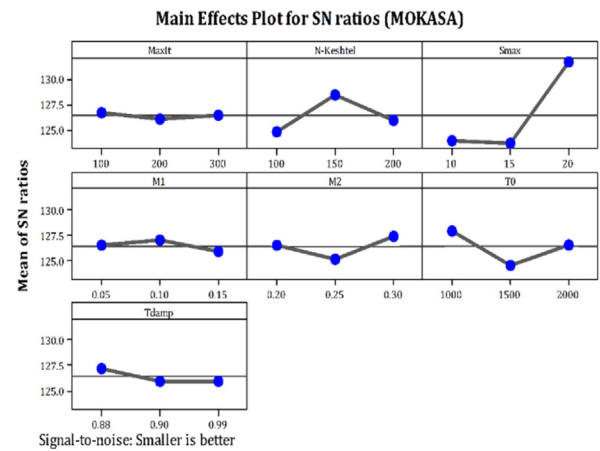


Fig. 12. Signal to Noise ratio plot for MOKASA.

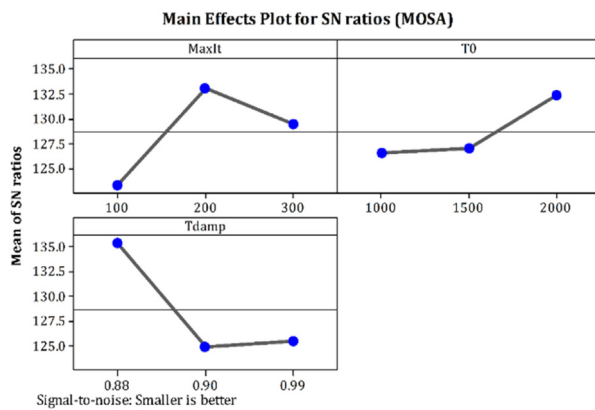


Fig. 10. Signal to Noise ratio plot for MOSA.

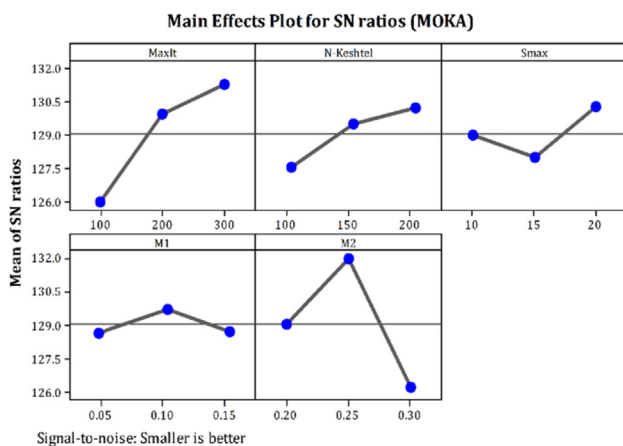


Fig. 11. Signal to Noise ratio plot for MOKA.

results of them as the average of all runs. Fig. 13 is related to problems 4, 9, and 14 as representative of different problem sizes.

Fig. 13 shows that obtained solutions of metaheuristic algorithms are significantly similar to each other. However, concerning the total cost, MOKASA, in small-size problems, NSGA-II in medium-size problems, and MOKA and MOKASA in large-size problem has better solutions. On the other hand, MOSA remarkably performed rather than other algorithms in demand coverage.

The result of five performance metrics is demonstrated in Table 5. Firstly, we convert all the metrics value to Relative Deviation Index (RDI) by using Eq. (20):

$$RDI = \frac{|S_{Alg} - S_{best}|}{S_{max} - S_{min}} \quad (20)$$

where S_{Alg} is the value attained by performance metric, S_{best} is the best value of performance metric among the applied metaheuristics. The means plot and LSD for each problem size are thoroughly explained in relevant sections.

Besides the abovementioned tool, we use two nonparametric statistical tests. Generally, metaheuristic algorithms have stochastic traits, so nonparametric statistical tests are mandatory for a more precise analysis of archived solutions by algorithm and comparison [78]. If the nonparametric statistical test only compares two algorithms, they label as pairwise comparisons. One of the appreciated pairwise nonparametric tests is Wilcoxon signed-rank test which we conduct in our study. As a post hoc test, we implement the Holm test. But, if they compare more than two algorithms, they define as multiple comparisons. The Friedman test is of multiple comparison tests, which is applied here [79]. Table 6 encompasses required definitions of terms associated with statistical tests; however, the detailed information can be found in Derrac et al. [79].

6.3.1. Small-size problems

According to Fig. 14, MOSA is leading in terms of SNS, CPU, and HV, though MOKA and MOKASA are better, respectively, in terms of MID and MS.

To implement Wilcoxon signed ranked test, we use HV values for small-size problems and run the test with a statistical significance level (α) of 0.05 using SPSS software. Table 7 presents the result of the Wilcoxon test. P-values for Wilcoxon tests and Holm tests in each comparison set are less than the significance level (α) of 0.05.

Finally, we did multiple statistical comparisons using the Friedman test for the small-size problem with a statistical significance level (α) of 0.05 using SPSS. This test is performed based on all performance metrics, and Table 8 shows the result of the Friedman test. Results state that MOSA has superior performance in all metrics than other algorithms except in HV that MOKA precedes other algorithms. It is worthwhile to mention that p-values in all tests are less than the significance level (α) of 0.05.

Table 5
Metaheuristics evaluation metrics value.

(a) Small sizes																					
Test No.	MID				MS				SNS				CPU Time				HV				
	NSGA-II	MOKA	MOSA	MOKASA	NSGA-II	MOKA	MOSA	MOKASA	NSGA-II	MOKA	MOSA	MOKASA	NSGA-II	MOKA	MOSA	MOKASA	NSGA-II	MOKA	MOSA	MOKASA	
Small	1	3.61	3.60	3.36	3.36	2.38E+07	6.58E+06	1.32E+07	5.11E+06	5.64E+06	4.53E+06	5.95E+06	2.04E+06	70.37	140.88	24.83	167.74	2.38E+07	6.58E+06	1.32E+07	5.11E+06
	2	1.74	1.49	1.56	1.74	3.25E+07	3.18E+07	3.77E+07	3.17E+07	1.73E+07	1.84E+07	1.59E+07	1.31E+07	106.84	171.19	28.61	250.27	3.25E+07	3.18E+07	3.77E+07	3.17E+07
	3	1.42	1.07	1.14	1.35	3.96E+07	3.63E+07	4.11E+07	4.35E+07	2.42E+07	2.30E+07	2.64E+07	2.06E+07	234.59	331.41	56.28	342.80	3.96E+07	3.63E+07	4.11E+07	4.35E+07
	4	1.40	1.19	1.09	1.05	1.34E+08	1.14E+08	1.35E+08	1.55E+08	5.83E+07	6.87E+07	5.05E+07	6.35E+07	245.71	501.18	46.74	298.67	1.34E+08	1.14E+08	1.55E+08	1.35E+08
	5	1.56	1.69	1.46	1.76	1.93E+08	1.76E+08	1.99E+08	2.02E+08	1.14E+08	1.22E+08	1.15E+08	1.24E+08	257.79	447.30	61.51	625.86	1.93E+08	1.76E+08	2.02E+08	1.99E+08
Average	1.95	1.81	1.72^a	1.85	8.48E+07	7.30E+07	8.52E+07	8.75E+07^a	4.39E+07	4.72E+07^a	4.28E+07	4.47E+07	183.06	318.39	43.59^a	337.07	8.48E+07	7.30E+07	8.98E+07^a	8.29E+07	
(b) Medium sizes																					
Test No.	MID				MS				SNS				CPU Time				HV				
	NSGA-II	MOKA	MOSA	MOKASA	NSGA-II	MOKA	MOSA	MOKASA	NSGA-II	MOKA	MOSA	MOKASA	NSGA-II	MOKA	MOSA	MOKASA	NSGA-II	MOKA	MOSA	MOKASA	
Medium	6	3.50	3.49	3.33	3.57	2.04E+08	2.13E+08	2.25E+08	2.14E+08	1.37E+08	1.39E+08	1.39E+08	1.31E+08	362.46	1070.63	88.66	533.99	2.04E+08	2.13E+08	2.14E+08	2.25E+08
	7	1.56	1.30	1.21	1.23	3.13E+08	3.16E+08	3.69E+08	3.53E+08	2.46E+08	2.52E+08	2.63E+08	2.29E+08	712.17	1478.15	177.49	779.78	3.13E+08	3.16E+08	3.53E+08	3.69E+08
	8	2.22	2.53	2.31	2.26	3.87E+08	3.43E+08	4.56E+08	4.82E+08	2.93E+08	2.84E+08	2.99E+08	2.92E+08	657.79	1539.59	223.29	1228.82	3.87E+08	3.43E+08	4.82E+08	4.56E+08
	9	1.40	1.04	1.09	1.36	7.48E+08	6.16E+08	5.26E+08	5.05E+08	6.86E+08	5.85E+08	6.56E+08	6.80E+08	688.03	2351.01	179.85	2050.09	7.48E+08	6.16E+08	5.05E+08	5.26E+08
	10	2.58	2.37	2.44	2.43	8.51E+08	6.63E+08	7.35E+08	8.31E+08	7.41E+08	5.64E+08	7.90E+08	6.19E+08	913.72	2277.87	212.78	2313.45	8.51E+08	6.63E+08	8.31E+08	7.35E+08
Average	2.25	2.15	2.08^a	2.17	5.01E+08^a	4.30E+08	4.62E+08	4.77E+08	4.21E+08	3.65E+08^a	4.29E+08	3.90E+08	666.83	1743.45	176.41^a	1381.23	5.01E+08^a	4.30E+08	4.77E+08	4.62E+08	
(c) Large sizes																					
Test No.	MID				MS				SNS				CPU Time				HV				
	NSGA-II	MOKA	MOSA	MOKASA	NSGA-II	MOKA	MOSA	MOKASA	NSGA-II	MOKA	MOSA	MOKASA	NSGA-II	MOKA	MOSA	MOKASA	NSGA-II	MOKA	MOSA	MOKASA	
Large	11	1.57	1.42	1.51	1.75	1.56E+09	1.17E+09	1.10E+09	1.33E+09	9.51E+08	1.05E+08	1.41E+09	9.30E+08	1261.84	3221.06	402.03	1975.52	1.56E+09	1.17E+09	1.10E+09	1.33E+09
	12	2.13	1.89	1.92	1.99	1.92E+09	1.87E+09	2.00E+09	1.82E+09	1.21E+09	1.34E+09	1.56E+09	1.39E+09	1493.99	3163.65	418.55	2390.81	1.92E+09	1.87E+09	2.00E+09	1.82E+09
	13	0.97	1.25	0.90	0.96	2.11E+09	2.73E+09	2.47E+09	2.60E+09	1.64E+09	1.51E+09	1.77E+09	1.77E+09	2674.83	7843.67	770.52	10142.84	2.11E+09	2.73E+09	2.47E+09	2.60E+09
	14	1.16	1.40	1.22	1.39	1.95E+09	2.75E+09	2.57E+09	1.98E+09	1.81E+09	1.79E+09	1.99E+09	1.88E+09	4560.31	10105.33	1447.79	12570.43	1.95E+09	2.75E+09	2.57E+09	1.98E+09
	15	2.15	1.96	1.82	1.91	1.61E+09	1.79E+09	1.72E+09	1.64E+09	1.96E+09	1.82E+09	1.97E+09	1.94E+09	9673.44	16719.78	2015.00	18167.51	2.66E+09	2.80E+09	3.29E+09	3.44E+09
Average	1.60	1.58	1.47^a	1.60	1.56E+09	1.17E+09	1.10E+09	1.33E+09^a	1.51E+09	1.31E+09	1.74E+09^a	1.58E+09	3932.88	8210.70	1010.78^a	9049.42	2.04E+09	2.26E+09^a	2.29E+09	2.23E+09	

^aBest performance.

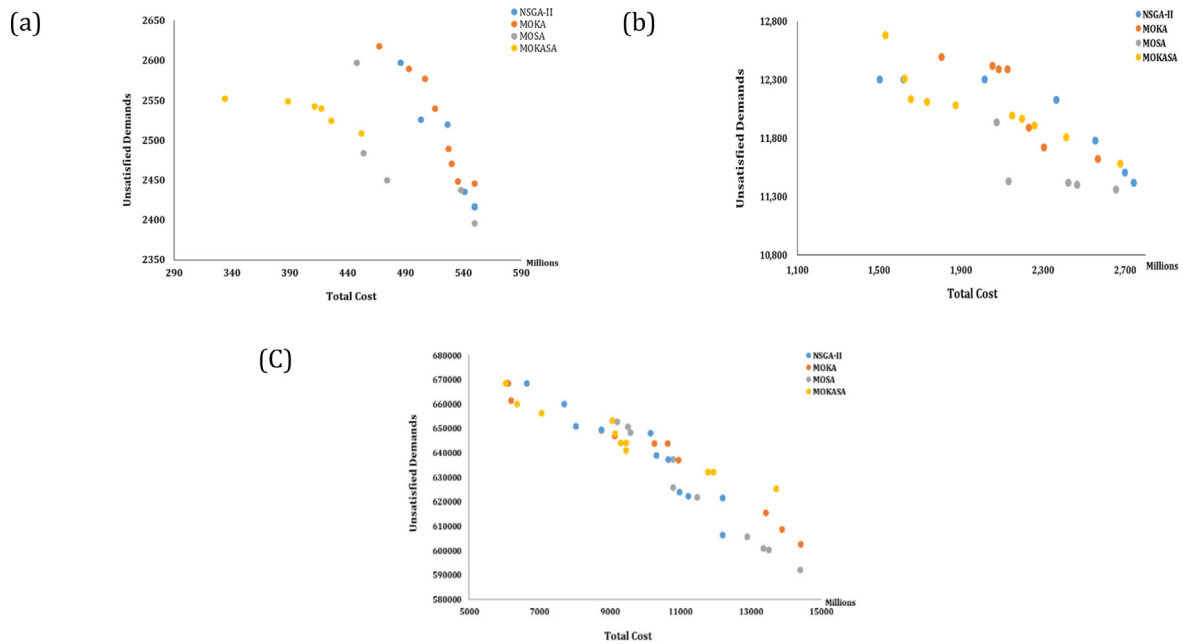


Fig. 13. Pareto frontier solutions related to: (a) Problem No. 4 (small-size) (b) Problem No. 9 (medium-size) (c) Problem No. 14 (large-size).

Table 6

Definition of statistical test terms.

Terms	Definition
The null hypothesis (H_0)	Declares that two metaheuristics have no difference.
alternative hypothesis (H_1)	Declares that two metaheuristics have differences.
Statistical significance level (α)	The probability of mistakenly rejecting H_0 . For p -value, less than α H_0 is rejected.
Family-Wise Error Rate (FWER)	The probability of rejecting a correct H_0 by at least one comparison test.
Post hoc test	The test examines and controls FWER.

Table 7

Wilcoxon signed the ranked test according to HV values for small-size problems.

Comparison	P-value (Wilcoxon test)	P-value (Holm test)
NSGA-II versus MOKA	.016	.022
NSGA-II versus MOSA	.029	.036
NSGA-II versus MOKASA	.038	.045
MOKA versus MOSA	.019	.028
MOKA versus MOKASA	.025	.030
MOSA versus MOKASA	.009	.014

Table 9

Wilcoxon signed the ranked test according to HV values for medium-size problems.

Comparison	P-value (Wilcoxon test)	P-value (Post-hoc test)
NSGA-II versus MOKA	.016	.022
NSGA-II versus MOSA	.036	.040
NSGA-II versus MOKASA	.015	.023
MOKA versus MOSA	.014	.018
MOKA versus MOKASA	.021	.031
MOSA versus MOKASA	.032	.035

6.3.2. Medium-size problems

Fig. 15 displays the means plot and LSD for medium-size problems. It can be concluded that MS, SNS, and CPU means plot and LSD, MOSA outperformed others. In terms of MID and HV, MOKA and MOKASA had better performance in comparison with other algorithms.

The result of the Wilcoxon test is demonstrated in Table 9. Like small-size problems, Wilcoxon signed a ranked test applied using HV values for medium-size problems with a statistical significance level (α) of 0.05 using SPSS software. P-values for

Wilcoxon tests and Holm tests are less than 0.05, so it determined that there is a difference between the two metaheuristics in each set.

Friedman test for medium-size problems with a significance level (α) of 0.05 using SPSS was carried out. All performance metrics have participated in this test for multiple comparisons, and Table 10 shows the achieved results. Excluding SNS that MOKA has been surpassed, results assert that MOSA has been at the top in all performance metrics.

Table 8

The Friedman ranks performance metrics for small-size problems.

Meta-heuristics	MID	Rank _{MID}	MS	Rank _{MS}	SNS	Rank _{SNS}	CPU	Rank _{CPU}	HV	Rank _{HV}
NSGA-II	3.20	3	2.60	2	2.65	2	2.45	2	2.40	3
MOSA	2.01	1	3.01	1	3.63	1	1.31	1	2.60	2
MOKA	2.20	2	1.65	4	1.01	4	3.10	3	3.32	1
MOKASA	2.32	4	2.34	3	2.42	3	3.32	4	2.12	4
P-value		.002		.005		.011		.000		.000

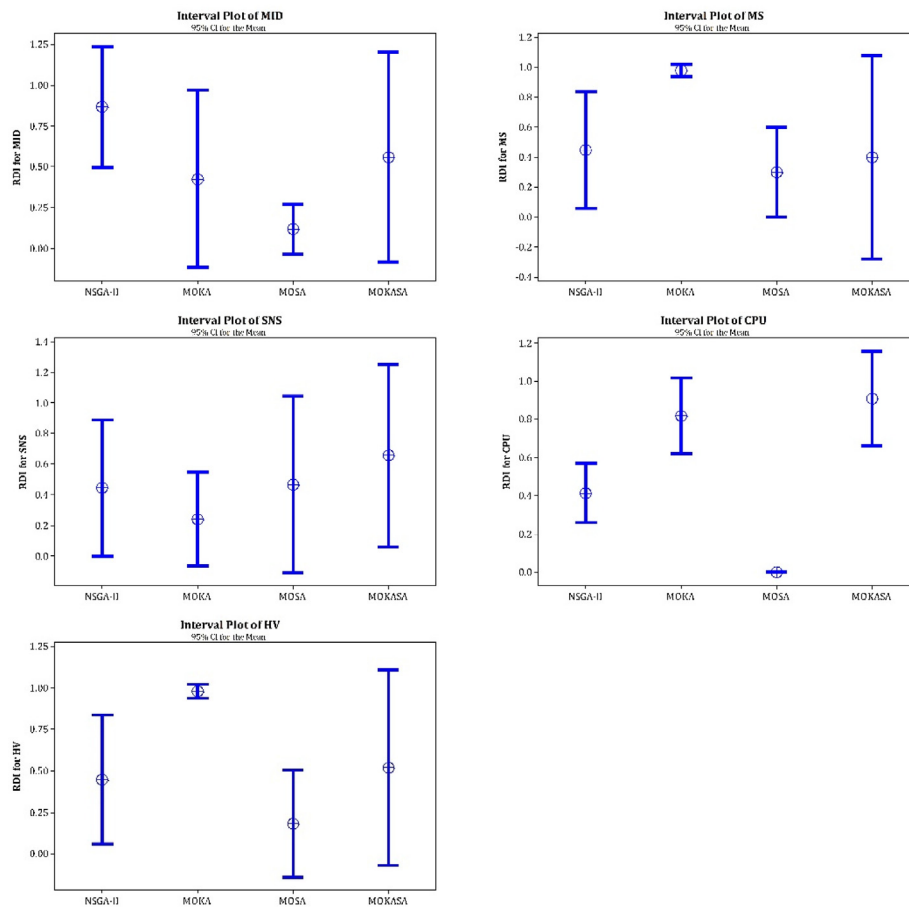


Fig. 14. Comparison of performance metrics for small-size problems.

Table 10
The Friedman ranks performance metrics for small-size problems.

Meta-heuristics	MID	Rank _{MID}	MS	Rank _{MS}	SNS	Rank _{SNS}	CPU	Rank _{CPU}	HV	Rank _{HV}
NSGA-II	2.05	2	2.43	2	2.04	3	2.25	2	2.12	3
MOSA	1.91	1	3.22	1	2.61	2	1.05	1	3.40	1
MOKA	2.62	4	1.78	4	3.31	1	2.61	3	1.52	4
MOKASA	3.42	3	2.41	3	1.24	4	3.38	4	2.81	2
P-value	.008		.001		.002		.000		.000	

6.3.3. Large-size problems

Here, the performance of large-size problems is evaluated through previously mentioned metrics. Firstly, the means plot and LSD are presented in Fig. 16. It reveals that MOSA had overcome other algorithms in terms of MS, SNS, CPU, and HV. But, in terms of MID, MOKASA is better than the others.

Large-size problems are statistically compared using Wilcoxon signed ranked test. In this test, HV values for large-size problems are considered and run the test with a significance level (α) of 0.05. The result illustrated in Table 11 for the Wilcoxon test, and Holm test is less than the significance level (α) of 0.05. As a result, there is a difference between each pair of algorithms. Table 12 shows the results of the Friedman test for the large-size problem with a statistical significance level (α) of 0.05. It can be comprehended that MOSA has superior performance in all metrics. The obtained p -value in all tests is less than 0.05.

In conclusion, the analysis of performance metrics for each problem size affirms that MOSA has a better performance compared to other algorithms.

Table 11

Wilcoxon signed the ranked test according to HV values for large-size problems.

Comparison	P-value (Wilcoxon test)	P-value (Post-hoc test)
NSGA-II versus MOKA	.007	.012
NSGA-II versus MOSA	.005	.015
NSGA-II versus MOKASA	.013	.023
MOKA versus MOSA	.021	.032
MOKA versus MOKASA	.018	.026
MOSA versus MOKASA	.012	.020

6.4. Sensitivity analyses

Here, we investigate the sensitivity analyses of parameter changes' effect on the proposed model's objective function values. In previous sections, MOSA is found as the most superior algorithm. Hence, MOSA is selected as the algorithm used for sensitivity analysis purposes using medium size problem number 9 in Table 2. The first experiment evaluates the impact of storage capacity, distributor capacity, and PPE production capacity on the objective functions. In this experiment, the range of storage capacity, distributor capacity, and PPE production capacity change

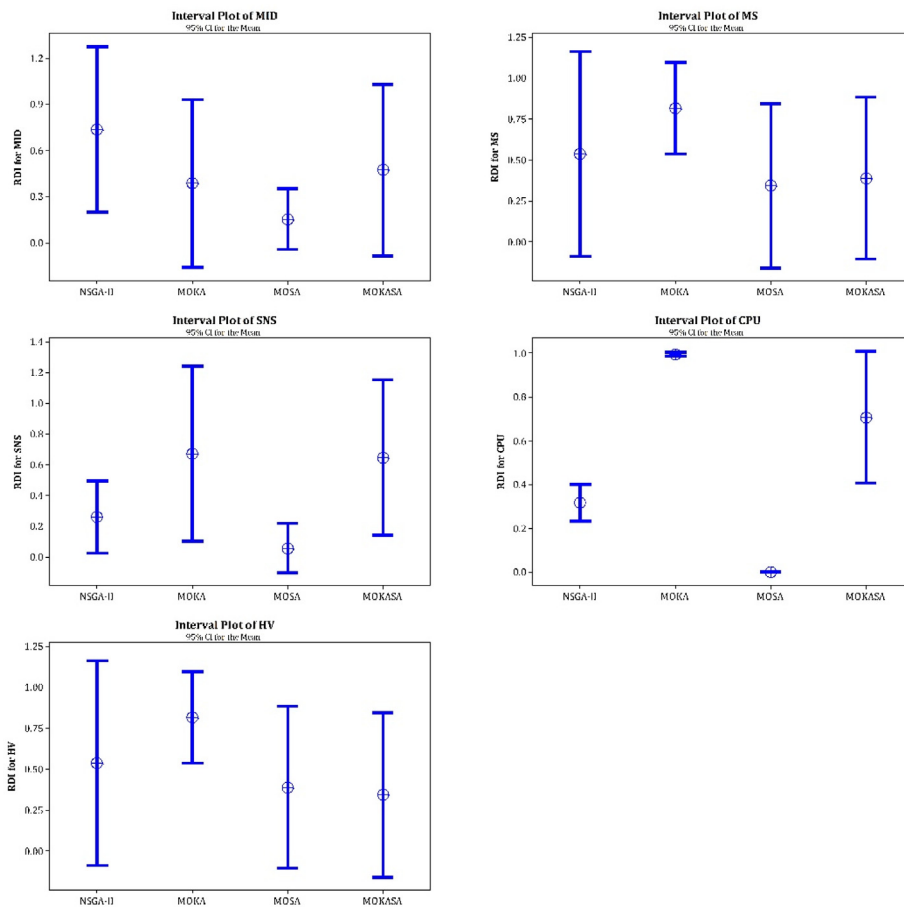


Fig. 15. Comparison of performance metrics for medium-size problems.

Table 12

The Friedman ranks performance metrics for large-size problems.

Meta-heuristics	MID	Rank _{MID}	MS	Rank _{MS}	SNS	Rank _{SNS}	CPU	Rank _{CPU}	HV	Rank _{HV}
NSGA-II	3.55	4	3.35	2	2.88	2	2.00	2	1.22	4
MOSA	2.04	2	3.65	1	3.65	1	1.09	1	3.83	1
MOKA	1.87	1	2.87	3	1.45	4	3.13	3	2.11	3
MOKASA	3.45	3	1.54	4	2.13	3	3.88	4	2.83	2
P Value	.011		.000		.003		.000		.001	

Table 13

The results of sensitivity analysis for the first experiment.

#Test	S_c	$Caps_{ict}$	$Capd_j$	Z_1	Z_2
T1	1	20	300	2,144,777,892	4700
T2	1.25	28	400	2,288,917,669	4854
T3	1.5	36	500	2,403,215,923	5907
T4	2	40	600	2,625,518,468	6988

from the lowest value to the highest value in four test problems. Afterward, test problems are solved using the MOSA algorithm, and the results are reported in Table 13. Fig. 17 exhibits that both objective functions Z_1 and Z_2 increase as the capacity and storage parameters have positive growth.

The second experiment monitors how the treatment capacity of the medical center and population of the region affects the behavior of total cost of supply chain and demand shortage. Similar to the previous experiment, this experiment considers the lowest and highest value of both parameters. For the designed test problems, the achieved outputs of MOSA for the second experiment are presented in Table 14. Furthermore, Fig. 18 emphasizes that

Table 14

The results of sensitivity analysis for the second experiment.

#Test	F_h	Pop	Z_1	Z_2
T1	100	1000	2,212,085,021	4711
T2	200	5000	2,428,290,551	5872
T3	400	10000	2,864,609,379	7851
T4	600	20000	3,153,300,213	9618

the total cost of supply chain and demand shortage are increased while the capacity of the medical center and population of the region significantly raised.

The third experiment is founded on the behavior of objective functions influenced by variation of recovery and death rate of patients. We consider a wide range for the death rate, from the lowest to the highest, in four experiments, and utilize the MOSA algorithm to solve these test problems. Table 15 and Fig. 19 point out that total cost and unsatisfied demand in the supply chain network have considerably positive relations.

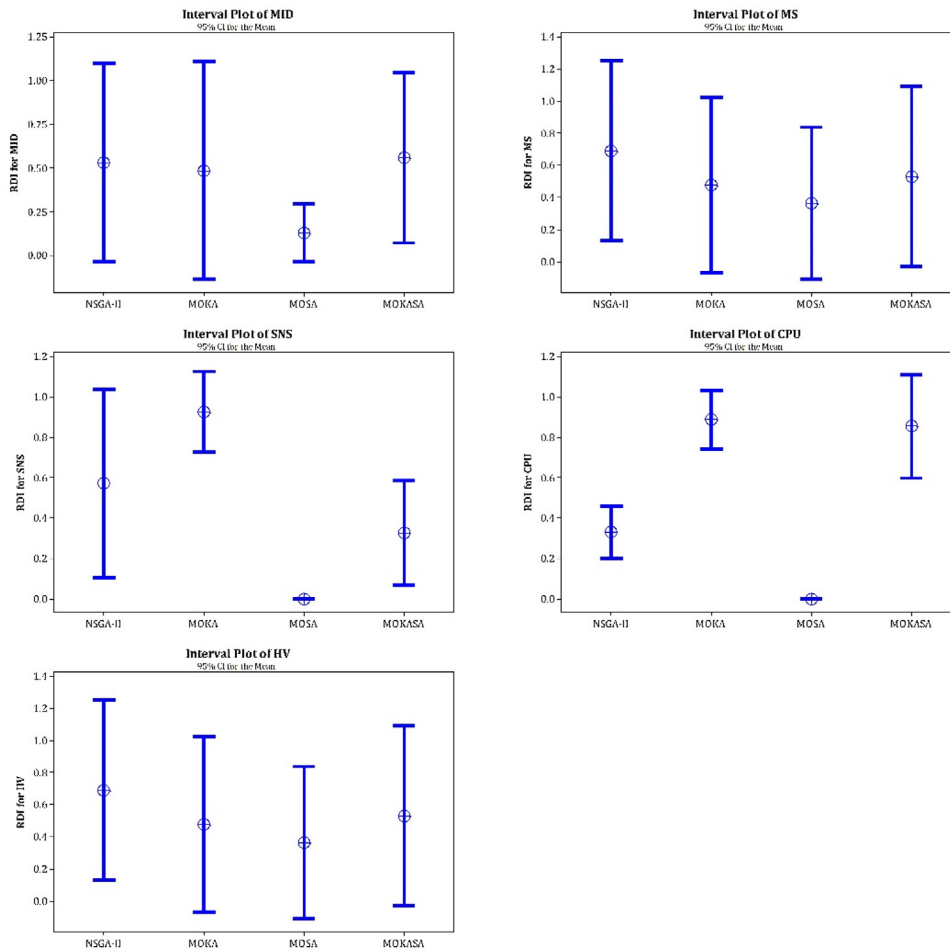


Fig. 16. Comparison of performance metrics for large-size problems.

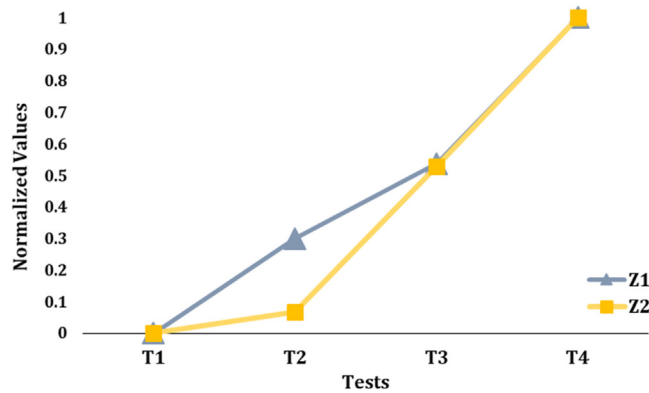


Fig. 17. Objective functions behavior based on the first experiment.

Table 15

The results of sensitivity analysis for the third experiment.

#Test	RP_{ht}	DP_{ht}	Z_1	Z_2
T1	0.10	0.10	2,112,048,000	4751
T2	0.15	0.15	2,223,809,174	4809
T3	0.30	0.20	2,345,978,529	5310
T4	0.45	0.30	2,412,048,000	6015

7. Conclusion

A relief SC network for the pandemic situation such as COVID-19 was designed in this paper. We modeled our proposed SC by using a multi-objective mathematical approach. We tried to investigate and analyze the total cost of the PPE SC and shortage throughout the network. Four multi-objective metaheuristic algorithms were applied, including MOKA, MOSA, NSGA-II, and MOKASA, to investigate and endorse the model's applicability. Afterward, the Taguchi method was used as a tuning assistant in this study to find the best level for the algorithms' parameters

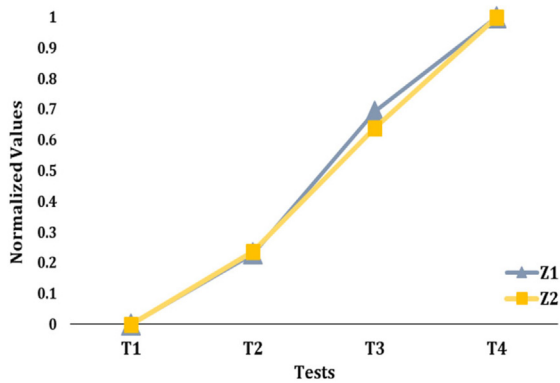


Fig. 18. Objective functions behavior based on the second experiment.

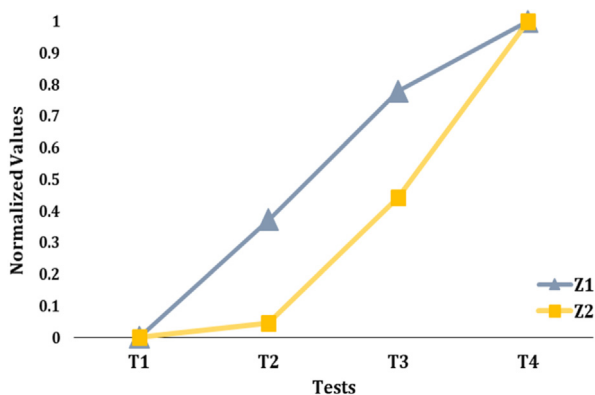


Fig. 19. Objective functions behavior based on the third experiment.

results achieving better performance. Among the fifteen developed test problems, the third test problem is inspired by a real case in Khuzestan province in southern Iran. Then, five evaluation criteria, MID, MS, SNS, HV, and CPU time, were utilized. Considering the evaluation criteria, each algorithm showed different behaviors, but, totally, we can conclude that MOSA showed better performance for the problems we studied in this work.

In this study, we confronted a few limitations which they could be overcome for future researches. Data gathering was the critical limitation in this work. As we earlier alleged, healthcare systems and organizations control the tough situation during the pandemic and try to prevent more casualties; therefore, they could not provide valid data. In future studies, researchers can access more valid data that might bring about closer solutions to reality. Another limitation of this study is that sustainability assumptions should be informed especially environmental and social aspects. In this study, the proposed model has not considered the problem in stochastic and uncertainty settings. Nevertheless, the model might be formulated with uncertainty constraints or parameters.

In general, we suggest the researchers for future studies to design the proposed PPE supply chain model tailored to the specific traits related to other countries' conditions and constraints, improve the proposed model by considering the vital aspect of sustainability, and formulate stochastic models for the PPE supply chain to satisfy the network's demand flow.

CRedit authorship contribution statement

Behzad Mosallanezhad: Investigation, Software, Data curation, Formal analysis. **Vivek Kumar Chouhan:** Conceptualization,

Investigation, Formal analysis, Writing – original draft, Visualization. **Mohammad Mahdi Paydar:** Supervision, Methodology, Validation, Writing – review & editing. **Mostafa Hajiaghaei-Keshteli:** Supervision, Methodology, Validation, Writing – review & editing.

Declaration of competing interest

The authors declare that they have no known competing financial interests or personal relationships that could have appeared to influence the work reported in this paper.

Appendix. Linearization of the second objective function

In Eq. (2), nonlinearity is discernible, so to overcome this issue, we use Eq. (A.1) instead of Eq. (2) and also add constraint (A.2) to the constraint sets.

$$\text{Min } Z_2 = \sum_c \sum_t \varphi_{ct} \tag{A.1}$$

$$\varphi_{ct} \geq B_{hct} \quad \forall h, c, t \tag{A.2}$$

References

- [1] World Health Organization, Rational use of personal protective equipment for coronavirus disease (COVID-19): interim guidance, in: 27th February 2020, No. WHO/2019-NCov/IPCPPE_use/2020.1, World Health Organization, 2020.
- [2] L. Cirrincione, F. Plescia, C. Ledda, V. Rapisarda, D. Martorana, R.E. Moldovan, et al., COVID-19 pandemic: prevention and protection measures to be adopted at the workplace, Sustainability 12 (9) (2020) 3603.
- [3] C. Sohrabi, Z. Alsafi, N. O'Neill, M. Khan, A. Kerwan, A. Al-Jabir, et al., World Health Organization declares global emergency: A review of the 2019 novel coronavirus (COVID-19), Int. J. Surg. 76 (2020) 71–76.
- [4] S.M. Hosseini, M.M. Paydar, M. Hajiaghaei-Keshteli, Recovery solutions for ecotourism centers during the Covid-19 pandemic: Utilizing Fuzzy DEMATEL and Fuzzy VIKOR methods, Expert Syst. Appl. (2021) 115594.
- [5] Y. Cao, Q. Li, J. Chen, X. Guo, C. Miao, H. Yang, et al., Hospital emergency management plan during the COVID-19 epidemic, Acad. Emerg. Med. 27 (4) (2020) 309–311.
- [6] E. Livingston, A. Desai, M. Berkwitz, Sourcing personal protective equipment during the COVID-19 pandemic, JAMA (2020).
- [7] Z. Ghaffari, M.M. Nasiri, A. Bozorgi-Amiri, A. Rahbari, Emergency supply chain scheduling problem with multiple resources in disaster relief operations, Transportmetrica A: Transp. Sci. 16 (3) (2020) 930–956.
- [8] L.-M. Jensen, S. Hertz, The coordination roles of relief organisations in humanitarian logistics, Int. J. Logist. Res. Appl. 19 (5) (2016) 465–485.
- [9] N. Haghjoo, R. Tavakkoli-Moghaddam, H. Shahmoradi-Moghadam, Y. Rahimi, Reliable blood supply chain network design with facility disruption: A real-world application, Eng. Appl. Artif. Intell. 90 (2020) 103493.
- [10] M.D. Garvey, S. Carnovale, The rippled newsvendor: A new inventory framework for modelling supply chain risk severity in the presence of risk propagation, Int. J. Prod. Econ. (2020) 107752.
- [11] D. Ivanov, A. Dolgui, Viability of intertwined supply networks: extending the supply chain resilience angles towards survivability. A position paper motivated by COVID-19 outbreak, Int. J. Prod. Res. (2020) 1–12.
- [12] J.-D. Hong, K.-Y. Jeong, K. Feng, Emergency relief supply chain design and trade-off analysis, J. Humanit. Logist. Supply Chain Manag. (2015).
- [13] L.F. Escudero, J.F. Monge, D.R. Morales, On the time-consistent stochastic dominance risk averse measure for tactical supply chain planning under uncertainty, Comput. Oper. Res. 100 (2018) 270–286.
- [14] M. Fattahi, K. Govindan, E. Keyvanshokoo, A multi-stage stochastic program for supply chain network redesign problem with price-dependent uncertain demands, Comput. Oper. Res. 100 (2018) 314–332.
- [15] A. Abdi, A. Abdi, A.M. Fathollahi-Fard, M. Hajiaghaei-Keshteli, A set of calibrated metaheuristics to address a closed-loop supply chain network design problem under uncertainty, Int. J. Syst. Sci.: Oper. Logist. 8 (1) (2021) 23–40.
- [16] A.S. Safaei, S. Farsad, M.M. Paydar, Emergency logistics planning under supply risk and demand uncertainty, Oper. Res. (2018) 1–24.
- [17] L. Ran, X. Chen, Y. Wang, W. Wu, L. Zhang, X. Tan, Risk factors of healthcare workers with corona virus disease 2019: A retrospective cohort study in a designated hospital of wuhan in china, Clin. Infect. Dis. (2020).
- [18] X. Wang, Y. Wu, L. Liang, Z. Huang, Service outsourcing and disaster response methods in a relief supply chain, Ann. Oper. Res. 240 (2) (2016) 471–487.

- [19] A. Nagurney, L.S. Nagurney, A mean-variance disaster relief supply chain network model for risk reduction with stochastic link costs, time targets, and demand uncertainty, in: Paper Presented at the International Conference on Dynamics of Disasters, 2016.
- [20] R. Mohammadi, S.F. Ghomi, F. Jolai, Prepositioning emergency earthquake response supplies: A new multi-objective particle swarm optimization algorithm, *Appl. Math. Model.* 40 (9–10) (2016) 5183–5199.
- [21] Y. Zhou, J. Liu, Y. Zhang, X. Gan, A multi-objective evolutionary algorithm for multi-period dynamic emergency resource scheduling problems, *Transp. Res. E* 99 (2017) 77–95.
- [22] A. Jha, D. Acharya, M. Tiwari, Humanitarian relief supply chain: a multi-objective model and solution, *Sādhanā* 42 (7) (2017) 1167–1174.
- [23] N. Al Theeb, C. Murray, Vehicle routing and resource distribution in post-disaster humanitarian relief operations, *Int. Trans. Oper. Res.* 24 (6) (2017) 1253–1284.
- [24] X. Li, R. Batta, C. Kwon, Effective and equitable supply of gasoline to impacted areas in the aftermath of a natural disaster, *Soc.-Econ. Plann. Sci.* 57 (2017) 25–34.
- [25] C. Cao, C. Li, Q. Yang, Y. Liu, T. Qu, A novel multi-objective programming model of relief distribution for sustainable disaster supply chain in large-scale natural disasters, *J. Cleaner Prod.* 174 (2018) 1422–1435.
- [26] A. Moreno, D. Alem, D. Ferreira, A. Clark, An effective two-stage stochastic multi-trip location-transportation model with social concerns in relief supply chains, *European J. Oper. Res.* 269 (3) (2018) 1050–1071.
- [27] S.A. Torabi, I. Shokr, S. Tofighi, J. Heydari, Integrated relief pre-positioning and procurement planning in humanitarian supply chains, *Transp. Res. E* 113 (2018) 123–146.
- [28] J.-D. Hong, K.-Y. Jeong, Goal programming and data envelopment analysis approach to disaster relief supply chain design, *Int. J. Logist. Syst. Manag.* 33 (3) (2019) 291–321.
- [29] D. Sarma, A. Das, U.K. Bera, A. Singh, Uncertain demand allocation with insufficient resource in disaster by using facebook disaster map under limited fund, in: International Conference on Information Technology and Applied Mathematics, Springer, Cham, 2019, pp. 567–578.
- [30] M. Aghajani, S.A. Torabi, J. Heydari, A novel option contract integrated with supplier selection and inventory pre-positioning for humanitarian relief supply chains, *Soc.-Econ. Plann. Sci.* (2020) 100780.
- [31] Z.D. Yenice, F. Samanlioglu, A multi-objective stochastic model for an earthquake relief network, *J. Adv. Transp.* 2020 (2020).
- [32] A. Barman, R. Das, P.K. De, Impact of COVID-19 in food supply chain: Disruptions and recovery strategy, *Curr. Res. Behav. Sci.* 2 (2021) 100017.
- [33] A. Belhadi, S. Kamble, C.J.C. Jabbour, A. Gunasekaran, N.O. Ndubisi, M. Venkatesh, Manufacturing and service supply chain resilience to the COVID-19 outbreak: Lessons learned from the automobile and airline industries, *Technol. Forecast. Soc. Change* 163 (2021) 120447.
- [34] T. Dai, M.H. Zaman, W.V. Padula, P.M. Davidson, Supply chain failures amid Covid-19 signal a new pillar for global health preparedness, 2021.
- [35] F. Motevalli-Taher, M.M. Paydar, Supply chain design to tackle coronavirus pandemic crisis by tourism management, *Appl. Soft Comput.* 104 (2021) 107217.
- [36] A. Zahedi, A. Salehi-Amiri, N.R. Smith, M. Hajiaghahi-Keshteli, Utilizing IoT to design a relief supply chain network for the SARS-COV-2 pandemic, *Appl. Soft Comput.* (2021) 107210.
- [37] K. Nikolopoulos, S. Punia, A. Schäfers, C. Tsinopoulos, C. Vasilakis, Forecasting and planning during a pandemic: COVID-19 growth rates, supply chain disruptions, and governmental decisions, *European J. Oper. Res.* 290 (1) (2021) 99–115.
- [38] A. Baveja, A. Kapoor, B. Melamed, Stopping Covid-19: A pandemic-management service value chain approach, *Ann. Oper. Res.* 289 (2020) 173–184.
- [39] K. Iyengar, S. Bahl, R. Vaishya, A. Vaish, Challenges and solutions in meeting up the urgent requirement of ventilators for COVID-19 patients, *Diabetes Metab. Syndr.: Clin. Res. Rev.* 14 (4) (2020) 499–501.
- [40] D. Chiaromonte, K. Maniatis, Security of supply, strategic storage and Covid19: Which lessons learnt for renewable and recycled carbon fuels, and their future role in decarbonizing transport? *Appl. Energy* 271 (2020) 115216.
- [41] M.S. Kumar, R.D. Raut, V.S. Narwane, B.E. Narkhede, Applications of industry 4.0 to overcome the COVID-19 operational challenges, *Diabetes Metab. Syndr.: Clin. Res. Rev.* 14 (5) (2020) 1283–1289.
- [42] A. Nagurney, Optimization of supply chain networks with inclusion of labor: Applications to Covid-19 pandemic disruptions, *Int. J. Prod. Econ.* 235 (2021a) 108080.
- [43] A. Nagurney, Supply chain game theory network modeling under labor constraints: Applications to the Covid-19 pandemic, *European J. Oper. Res.* (2021b).
- [44] A. Nagurney, Perishable food supply chain networks with labor in the COVID-19 pandemic, in: I.S. Kotsireas, A. Nagurney, P.M. Pardalos, A. Tsokas (Eds.), *Dynamics of Disasters: Impact, Risk, Resilience, and Solutions*, Springer International Publishing Switzerland, 2020.
- [45] A. Nagurney, M. Salarpour, J. Dong, P. Dutta, Competition for medical supplies under stochastic demand in the Covid-19 pandemic: A generalized nash equilibrium framework, in: Themistocles M. Rassias, Panos M. Pardalos (Eds.), *Nonlinear Analysis and Global Optimization*, Springer Nature AG, 2020 forthcoming.
- [46] S. Nandi, J. Sarkis, A.A. Hervani, M.M. Helms, Redesigning supply chains using blockchain-enabled circular economy and COVID-19 experiences, *Sustain. Prod. Consum.* 27 (2021) 10–22.
- [47] D. Ivanov, Predicting the impacts of epidemic outbreaks on global supply chains: A simulation-based analysis on the coronavirus outbreak (COVID-19/SARS-CoV-2) case, *Transp. Res. E* 136 (2020) 101922.
- [48] F. Goodarzian, A. Abraham, A.M. Fathollahi-Fard, A biobjective home health care logistics considering the working time and route balancing: a self-adaptive social engineering optimizer, *J. Comput. Des. Eng.* 8 (1) (2021a) 452–474.
- [49] B. Abbasi, M. Fadaki, O. Kokshagina, N. Saeed, P. Chhetri, Modeling vaccine allocations in the COVID-19 pandemic: A case study in australia, 2020, Available at SSRN 3744520.
- [50] M. Habibi-Kouchaksaraei, M.M. Paydar, E. Asadi-Gangraj, Designing a bi-objective multi-echelon robust blood supply chain in a disaster, *Appl. Math. Model.* 55 (2018) 583–599.
- [51] A. Mohamadi, S. Yaghoubi, M.S. Pishvae, Fuzzy multi-objective stochastic programming model for disaster relief logistics considering telecommunication infrastructures: a case study, *Oper. Res.* 19 (1) (2019) 59–99.
- [52] S.M. Shavarani, Multi-level facility location-allocation problem for post-disaster humanitarian relief distribution, *J. Humanit. Logist. Supply Chain Manag.* (2019).
- [53] M. Akbarpour, S.A. Torabi, A. Ghavamifar, Designing an integrated pharmaceutical relief chain network under demand uncertainty, *Transp. Res. E* 136 (2020) 101867.
- [54] Y. Li, J. Zhang, G. Yu, A scenario-based hybrid robust and stochastic approach for joint planning of relief logistics and casualty distribution considering secondary disasters, *Transp. Res. E* 141 (2020) 102029.
- [55] P. Ghasemi, K. Khalili-Damghani, A robust simulation-optimization approach for pre-disaster multi-period location-allocation-inventory planning, *Math. Comput. Simulation* 179 (2021) 69–95.
- [56] H. Molladavoodi, M.M. Paydar, A.S. Safaei, A disaster relief operations management model: a hybrid LP-GA approach, *Neural Comput. Appl.* 32 (4) (2020) 1173–1194.
- [57] R. Mousavi, A. Salehi-Amiri, A. Zahedi, M. Hajiaghahi-Keshteli, Designing a supply chain network for blood decomposition by utilizing social and environmental factor, *Comput. Ind. Eng.* (2021) 107501.
- [58] M. Hajiaghahi-Keshteli, S.M. Sajadifar, R. Haji, Determination of the economical policy of a three-echelon inventory system with (R, Q) ordering policy and information sharing, *Int. J. Adv. Manuf. Technol.* 55 (5–8) (2011) 831–841.
- [59] A. Cheraghali-pour, M.M. Paydar, M. Hajiaghahi-Keshteli, An integrated approach for collection center selection in reverse logistics, *Int. J. Eng.* 30 (7) (2017) 1005–1016.
- [60] V.K. Chouhan, S.H. Khan, M. Hajiaghahi-Keshteli, et al., Multi-facility-based improved closed-loop supply chain network for handling uncertain demands, *Soft Comput.* 24 (2020) 7125–7147, <http://dx.doi.org/10.1007/s00500-020-04868-x>.
- [61] B. Mosallanezhad, M. Hajiaghahi-Keshteli, C. Triki, Shrimp closed-loop supply chain network design, *Soft Comput.* (2021) 1–24.
- [62] K.P. Nurjanni, M.S. Carvalho, L. Costa, Green supply chain design: A mathematical modeling approach based on a multi-objective optimization model, *Int. J. Prod. Econ.* 183 (2017) 421–432.
- [63] H.K. Sarvestani, A. Zadeh, M. Seyfi, M. Rasti-Barzoki, Integrated order acceptance and supply chain scheduling problem with supplier selection and due date assignment, *Appl. Soft Comput.* 75 (2019) 72–83.
- [64] D. Sarma, A. Das, U.K. Bera, Uncertain demand estimation with optimization of time and cost using Facebook disaster map in emergency relief operation, *Appl. Soft Comput.* 87 (2020) 105992.
- [65] F. Goodarzian, H. Hosseini-Nasab, J. Muñuzuri, M.B. Fakhrazad, A multi-objective pharmaceutical supply chain network based on a robust fuzzy model: A comparison of meta-heuristics, *Appl. Soft Comput.* 92 (2020) 106331.
- [66] A.M. Fathollahi-Fard, A. Ahmadi, F. Goodarzian, N. Cheikhrouhou, A bi-objective home healthcare routing and scheduling problem considering patients' satisfaction in a fuzzy environment, *Appl. Soft Comput.* 93 (2020) 106385.
- [67] F. Goodarzian, A.A. Taleizadeh, P. Ghasemi, A. Abraham, An integrated sustainable medical supply chain network during COVID-19, *Eng. Appl. Artif. Intell.* 100 (2021b) 104188.
- [68] M. Hajiaghahi-Keshteli, M. Aminnayeri, Keshtel Algorithm (KA); a new optimization algorithm inspired by Keshtels' feeding, in: Proceeding in IEEE Conference on Industrial Engineering and Management Systems, 2013, pp. 2249–2253.

- [69] M. Hajiaghahi-Keshteli, M. Aminnayeri, Solving the integrated scheduling of production and rail transportation problem by Keshtel algorithm, *Appl. Soft Comput.* 25 (2014) 184–203.
- [70] A. Cheraghalipour, M.M. Paydar, M. Hajiaghahi-Keshteli, A bi-objective optimization for citrus closed-loop supply chain using Pareto-based algorithms, *Appl. Soft Comput.* 69 (2018) 33–59.
- [71] S. Kirkpatrick, C.D. Gelatt, M.P. Vecchi, Optimization by simulated annealing, *Science* 220 (1983) 671–680.
- [72] S. Golmohamadi, R. Tavakkoli-Moghaddam, M. Hajiaghahi-Keshteli, Solving a fuzzy fixed charge solid transportation problem using batch transferring by new approaches in meta-heuristic, *Electron. Notes Discrete Math.* 58 (2017) 143–150.
- [73] K. Deb, A. Pratap, S. Agarwal, T.A.M.T. Meyarivan, A fast and elitist multi-objective genetic algorithm: NSGA-II, *IEEE Trans. Evol. Comput.* 6 (2) (2002) 182–197.
- [74] J. Behnamian, S.F. Ghomi, Hybrid flowshop scheduling with machine and resource-dependent processing times, *Appl. Math. Model.* 35 (3) (2011) 1107–1123.
- [75] A.F. Fard, F. Gholian-Jouybari, M.M. Paydar, M. Hajiaghahi-Keshteli, A bi-objective stochastic closed-loop supply chain network design problem considering downside risk, *Ind. Eng. Manag. Syst.* 16 (3) (2017) 342–362.
- [76] E. Roghanian, A. Cheraghalipour, Addressing a set of meta-heuristics to solve a multi-objective model for closed-loop citrus supply chain considering CO₂ emissions, *J. Cleaner Prod.* 239 (2019) 118081.
- [77] G. Taguchi, *Introduction to quality engineering: designing quality into products and processes*, 1986.
- [78] N. Sahebjamnia, F. Goodarzi, M. Hajiaghahi-Keshteli, Optimization of multi-period three-echelon citrus supply chain problem, *J. Optim. Ind. Eng.* 13 (1) (2020) 39–53.
- [79] J. Derrac, S. García, D. Molina, F. Herrera, A practical tutorial on the use of nonparametric statistical tests as a methodology for comparing evolutionary and swarm intelligence algorithms, *Swarm Evol. Comput.* 1 (1) (2011) 3–18.